J. Fluid Mech. (1987), *vol.* 182, *pp.* 499–523
Printed in Great Britain

Nonlinear interactions of gravity–capillary waves: Lagrangian theory and effects on the spectrum

By KLAARTJE VAN GASTEL
Royal Netherlands Meteorological Institute, PO Box 201, 3730 AE De Bilt, The Netherlands†

(Received 1 January 1986 and in revised form 24 February 1987)

A weakly nonlinear inviscid theory describing the interactions within a continuous spectrum of gravity–capillary waves is developed. The theory is based on the principle of least action and uses a Lagrangian in wavenumber–time space. Advantages of this approach compared to the method of Valenzuela & Laing (1972) are much simplified mathematics and final equations and validity on a longer timescale. It is shown that much of the development of the spectrum under the influence of nonlinear terms can be understood without actually having to integrate the equations. To this end multiwave space, a new concept comparable with phase space, is introduced. Using multiwave space the magnitude of the nonlinear transfer is estimated and it is shown how the energy goes through the spectrum. Also it is predicted that at fixed wavenumbers, the smallest being 520 m^{-1}, finite peaks will arise in the spectrum. This is confirmed by numerical integrations. From the integrations it is also deduced that nonlinear interactions are at least as important to the development of the spectrum as wind growth. Finally it is shown numerically that the near-Gaussian statistics of the sea surface are unaffected by nonlinear interactions.

1. Introduction

Remote sensing of our seas, which has really taken flight over the last decade, gives a lot of information which the scientific world still has difficulty in interpreting correctly. One example of this is the images of bottom topography of shallow waters taken by microwave radar. An essential link in the imaging process is formed by gravity–capillary waves on the ocean surface. One of the problems in explaining bottom-topography images is that knowledge about the behaviour of these wavelets is incomplete, while part of what is known is still too intricate to be handled in a compound model (Phillips 1984).

This paper deals with gravity–capillary waves. I shall first give a brief review of the present level of our knowledge of them. This is done most easily in the context of the energy-balance equation (Willebrand 1975):

$$\left.\begin{aligned}\left[\frac{\partial}{\partial t}+\frac{\partial \Omega}{\partial \boldsymbol{k}}\frac{\partial}{\partial \boldsymbol{x}}-\frac{\partial \Omega}{\partial \boldsymbol{x}}\frac{\partial}{\partial \boldsymbol{k}}\right]A &= S_{\text{wind}}+S_{\text{visc}}+S_{\text{nl}}+S_{\text{br}},\\ \Omega &= \boldsymbol{k}\cdot\boldsymbol{U}+\omega.\end{aligned}\right\} \tag{1}$$

Here $A(\boldsymbol{k},\boldsymbol{x},t)$ denotes the action density, defined by $A = E/\omega$, E being the local energy density and ω the intrinsic frequency. Also, Ω is the apparent frequency, $\boldsymbol{U}$

† Present address: State University of Utrecht, Mathematical Institute, P.O. Box 80.010, 3508 TA Utrecht, The Netherlands.

the surface current and S stands for source or sink, respectively acting due to wind, viscosity, nonlinear interactions and breaking events. Actually all sources are coupled, but as an approximation they are dealt with separately (Komen, Hasselmann & Hasselmann 1984).

The damping due to viscosity is well known: $S_{\text{visc}} = -4\nu k^2 A$ (Phillips 1977, p. 52). The equations governing the energy input by wind are also familiar (Miles 1962; Valenzuela 1976), but it is only recently that a quick and accurate way to solve them has been found (van Gastel, Janssen & Komen 1985). We know very little of the causes and frequency of breaking of the waves (Phillips 1984) although Banner & Phillips (1974) have made some theoretical predictions. The nonlinear interactions in a spectrum of gravity–capillary waves have been calculated by Valenzuela & Laing (1972). A drawback of their method, which is based on Hasselmann's (1962) perturbation analysis, is that the resulting expressions for the interaction coefficients are complicated and cannot be understood physically; also the numerical computations necessary for quantitative results are delicate and lengthy. This is probably one of the reasons why the nonlinear interactions have never yet been included when solving the energy balance. As Longuet-Higgins (1976) puts it: 'there is obviously a need for a much simpler approach, more amenable to physical interpretation'.

The aim of this paper is to increase our knowledge of the nonlinear interactions in a continuous spectrum of gravity–capillary waves to such a level that an accurate description of these interactions can be used when solving the energy balance (1) for this part of the spectrum. This work can be divided into three steps: (i) mathematical derivation of the interaction equations; (ii) construction of a physical image of how the wavenumbers are related to each other by the resonance conditions; and (iii) study of the symmetries present within a triad. Point (ii) helps to make interpretations of numerical integrations possible and greatly increases their efficiency.

Analytical expressions for the nonlinear interactions in a continuous spectrum of gravity–capillary waves are obtained as the Euler–Lagrange equations for the Lagrangian in wavenumber–time space. An expansion is made in powers of the wave steepness. This method can be seen as a generalization to the continuous case of the method of Simmons (1969) or of that described by Whitham (1967) for resonant interactions. The advantages of using a Lagrangian or Hamiltonian formalism in this case are simpler mathematics, simpler final expressions and validity on a longer timescale. These advantages have been pointed out frequently in recent years (Miles & Salmon 1985; Henyey 1983).

To achieve point (ii) I introduce a new concept: the multiplet-wavevector space, multiwave space for short (a multiplet is a set of waves that together fulfill the resonance conditions). This concept can be compared with phase space in classical mechanics. Phase space tells us at a glance how physical space is interconnected by trajectories. Similarly, in multiwave space we see the interconnections in wavevector space due to the nonlinear interactions. The multiwave space is constructed explicitly for triad resonances between parallel gravity–capillary waves. In this case it is two-dimensional.

Point (iii), the use of symmetries, is straightforward. It is comparable with the way Hasselmann & Hasselmann (1981) use symmetries for four-wave interactions.

One of the gains of using multiwave space and symmetries is that resonance conditions and interaction coefficients need be solved only for part of the wavevector space, in the present case only for $k \leqslant (g/2T)^{\frac{1}{2}}$. Another gain is that it allows for a natural construction of a grid for numerical calculations, implying high accuracy. This grid follows the paths of the energy through the spectrum.

An energy balance containing nonlinear interactions is actually integrated. As initial states the spectra measured by Liu & Lin (1982) are used. A surprising phenomenon is encountered: the existence of preferred wavelengths, i.e. peaks in the energy spectrum. I explain the occurrence of these peaks using multiwave space.

As a sideline the issue of near Gaussianity of the sea surface is considered. The Gaussian approximation is essential to the weakly nonlinear theory underlying multiplet interactions. Davidson (1972) showed analytically for all processes dominated by three- or four-wave interactions that, if the initial sea surface is near Gaussian, the third cumulant, commonly related to phase-locking, goes to a constant. I show numerically that, for the cases considered, this constant is small.

2. The interaction equations

The equations for the surface elevation ζ are derived using the principle of least action. Nonlinear effects are included up to first order. The surface elevation is supposed to consist of a continuum of free gravity–capillary waves. Viscosity is neglected.

The action J can be written as

$$J = \int\int L \,\mathrm{d}x \,\mathrm{d}t. \tag{2}$$

For water waves the Lagrangian L is a function of the elevation ζ and the potential ϕ. For infinitely deep water it is given by (Simmons 1969; Luke 1967)

$$L = \tfrac{1}{2}g\zeta^2 + T[(1+\tilde{\nabla}\zeta\cdot\tilde{\nabla}\zeta)^{\frac{1}{2}} - 1] + \int_{-\infty}^{\zeta} (\tfrac{1}{2}\nabla\phi\cdot\nabla\phi + \dot{\phi})\,\mathrm{d}z. \tag{3}$$

Here g is the acceleration due to gravity and T the surface tension divided by the density. The derivatives are defined as follows:

$$\left.\begin{aligned} \dot{\phi} &= \frac{\partial}{\partial t}\phi, \quad \nabla\phi = \left(\frac{\partial\phi}{\partial x}, \quad \frac{\partial\phi}{\partial y}, \quad \frac{\partial\phi}{\partial z}\right), \\ \tilde{\nabla}\zeta &= \left(\frac{\partial\zeta}{\partial x}, \quad \frac{\partial\zeta}{\partial y}\right). \end{aligned}\right\} \tag{4}$$

The Lagrangian as presented in (3) is a function of horizontal space and time. To be able to perform the integration in the Lagrangian I apply a Fourier transform and substitute the dependence on the vertical for each mode:

$$\left.\begin{aligned} \zeta(\boldsymbol{x},t) &= \frac{1}{2\pi}\int \hat{\zeta}(\boldsymbol{k},t)\,\mathrm{e}^{-\mathrm{i}\boldsymbol{k}\cdot\boldsymbol{x}}\,\mathrm{d}\boldsymbol{k}, \\ \phi(\boldsymbol{x},z,t) &= \frac{1}{2\pi}\int \hat{\phi}(\boldsymbol{k},t)\,\mathrm{e}^{-\mathrm{i}\boldsymbol{k}\cdot\boldsymbol{x}+kz}\,\mathrm{d}\boldsymbol{k}, \\ k &= |\boldsymbol{k}|. \end{aligned}\right\} \tag{5}$$

A new Lagrangian $\hat{L}$ depending on wavenumber and time is defined by

$$J = \int\int \hat{L}\,\mathrm{d}\boldsymbol{k}\,\mathrm{d}t. \tag{6}$$

It can be given explicitly by assuming the waves to be of small, though finite amplitude, or, equivalently

$$\forall \boldsymbol{k}, t: \quad \hat{\zeta}(\boldsymbol{k}, t) = \epsilon \hat{\zeta}'(\boldsymbol{k}, t), \quad \hat{\phi}(\boldsymbol{k}, t) = \epsilon \hat{\phi}'(\boldsymbol{k}, t), \quad \hat{\zeta}' = O(1), \tag{7}$$

where ϵ is a small parameter proportional to the wave steepness. This assumption will be checked in §5. The primes will be dropped in the following. ϵ being small enables the Lagrangian $\hat{L}$ to be expanded in powers of ϵ. Using the identity

$$\int \mathrm{e}^{-\mathrm{i}\boldsymbol{k}\cdot\boldsymbol{x}} \, \mathrm{d}\boldsymbol{x} = 4\pi^2 \delta(\boldsymbol{k}) \tag{8}$$

this expansion becomes (here and in the following the dependence on t of all functions is not stated explicitly when no confusion can arise)

$$\begin{aligned} \hat{L}(\boldsymbol{k}, t) = \epsilon^2 [\tfrac{1}{2}(g + k^2 T)\, \hat{\zeta}(\boldsymbol{k})\, \hat{\zeta}(-\boldsymbol{k}) + \tfrac{1}{2} k \hat{\phi}(\boldsymbol{k})\, \hat{\phi}(-\boldsymbol{k}) + \dot{\hat{\phi}}(\boldsymbol{k})\, \hat{\zeta}(-\boldsymbol{k})] \\ + \epsilon^3 \tfrac{1}{4}\pi \int\int [(-\boldsymbol{k}\boldsymbol{k}' + kk')\, \hat{\phi}(\boldsymbol{k})\, \hat{\phi}(\boldsymbol{k}')\, \hat{\zeta}(\boldsymbol{k}'') \\ + k \dot{\hat{\phi}}(\boldsymbol{k})\, \hat{\zeta}(\boldsymbol{k}')\, \hat{\zeta}(\boldsymbol{k}'')] \, \delta(\boldsymbol{k} + \boldsymbol{k}' + \boldsymbol{k}'') \, \mathrm{d}\boldsymbol{k}' \, \mathrm{d}\boldsymbol{k}'' + O(\epsilon^4). \end{aligned} \tag{9}$$

The principle of least action states that physical realizations of the system are given by $\delta J = 0$. This condition can be transformed into a condition on the Lagrangian, as in the familiar Euler–Lagrange equations. To illustrate the method I use a simplified Lagrangian $\tilde{L}$; for the actual Lagrangian given by (9) the procedure is analogous. Let $\tilde{L}$ be a function of $\phi(\boldsymbol{k})$ and $\phi(-\boldsymbol{k})$. Then

$$\delta J = \int \tilde{L}[\phi(\boldsymbol{k}) + \tilde{\epsilon} u(\boldsymbol{k}), \phi(-\boldsymbol{k}) + \tilde{\epsilon} u(-\boldsymbol{k})] \, \mathrm{d}\boldsymbol{k} - \int \tilde{L}(\phi(\boldsymbol{k}), \phi(-\boldsymbol{k})) \, \mathrm{d}\boldsymbol{k}.$$

Here $\tilde{\epsilon}$ is a small parameter and u is a smooth function of $\boldsymbol{k}$ disappearing at the integration boundaries. Continuing:

$$\begin{aligned} \delta J &= \tilde{\epsilon} \int \left[\left(\frac{\partial}{\partial \phi(\boldsymbol{k})} \tilde{L}(\phi(\boldsymbol{k}), \phi(-\boldsymbol{k})) \right) u(\boldsymbol{k}) + \left(\frac{\partial}{\partial \phi(-\boldsymbol{k})} \tilde{L}(\phi(\boldsymbol{k}), \phi(-\boldsymbol{k})) \right) u(-\boldsymbol{k}) \right] \mathrm{d}\boldsymbol{k} \\ &= \tilde{\epsilon} \int \left[\frac{\partial}{\partial \phi(\boldsymbol{k})} (\tilde{L}(\phi(\boldsymbol{k}), \phi(-\boldsymbol{k})) + \tilde{L}(\phi(-\boldsymbol{k}), \phi(\boldsymbol{k}))) \right] u(\boldsymbol{k}) \, \mathrm{d}\boldsymbol{k}. \end{aligned}$$

Thus

$$\delta J = 0 \Leftrightarrow \frac{\partial}{\partial \phi(\boldsymbol{k})} [\tilde{L}(\phi(\boldsymbol{k}), \phi(-\boldsymbol{k})) + \tilde{L}(\phi(-\boldsymbol{k}), \phi(\boldsymbol{k}))] = 0.$$

Applying this procedure to the present Lagrangian $\hat{L}$ yields two equations as there are two independent functions $\hat{\zeta}$ and $\hat{\phi}$.

Using the substitution $\boldsymbol{k} \to -\boldsymbol{k}$ these equations can be written as

$$\left.\begin{aligned} \dot{\hat{\phi}}(\boldsymbol{k}) &= -(g + k^2 T)\, \hat{\zeta} - \epsilon \frac{1}{2\pi} \int\int [\tfrac{1}{2}(-\boldsymbol{k}'\boldsymbol{k}'' + \boldsymbol{k}'\boldsymbol{k}'')\, \hat{\phi}(\boldsymbol{k}')\, \hat{\phi}(\boldsymbol{k}'') \\ &\qquad + \boldsymbol{k}'' \dot{\hat{\phi}}(\boldsymbol{k}'')\, \hat{\zeta}(\boldsymbol{k}')] \, \delta(\boldsymbol{k} - \boldsymbol{k}' - \boldsymbol{k}'') \, \mathrm{d}\boldsymbol{k}' \, \mathrm{d}\boldsymbol{k}'', \\ \dot{\hat{\zeta}}(\boldsymbol{k}) &= k\hat{\phi} + \epsilon \frac{1}{2\pi} \int\int [(\boldsymbol{k}\boldsymbol{k}' + kk')\, \hat{\phi}(\boldsymbol{k}')\, \hat{\zeta}(\boldsymbol{k}'') \\ &\qquad - k \dot{\hat{\zeta}}(\boldsymbol{k}')\, \hat{\zeta}(\boldsymbol{k}'')] \, \delta(\boldsymbol{k} - \boldsymbol{k}' - \boldsymbol{k}'') \, \mathrm{d}\boldsymbol{k}' \, \mathrm{d}\boldsymbol{k}''. \end{aligned}\right\} \tag{10}$$

The zeroth-order or linear solutions are two independent functions oscillating with frequencies

$$\omega(\boldsymbol{k}) = (gk + k^3 T)^{\frac{1}{2}}. \tag{11}$$

These functions are the normal modes of the system. By eliminating $\hat{\phi}$ from (10) and transforming to these normal modes according to

$$\left.\begin{aligned}\hat{\zeta}(\boldsymbol{k},t) &= \alpha_+(t)\,\epsilon^{\mathrm{i}\omega(\boldsymbol{k})t}+\alpha_-(t)\,\epsilon^{-\mathrm{i}\omega(\boldsymbol{k})t},\\ \dot{\hat{\zeta}}(\boldsymbol{k},t) &= \mathrm{i}\omega(\boldsymbol{k})\,\alpha_+(t)\,\epsilon^{\mathrm{i}\omega(\boldsymbol{k})t}-\mathrm{i}\omega(\boldsymbol{k})\,\alpha_-(t)\,\epsilon^{-\mathrm{i}\omega(\boldsymbol{k})t},\end{aligned}\right\} \tag{12}$$

equations for the amplitudes of the modes are derived which are uncoupled at lowest order:

$$\begin{aligned}\frac{\partial}{\partial t}\alpha_\sigma = \frac{-\mathrm{i}k\epsilon}{8\pi\omega}\int\int\Big\{\sum_{\sigma'\sigma''}\Big[&-\frac{\boldsymbol{k}\boldsymbol{k}'+kk'}{kk'}\omega'_{\sigma'}(\omega'_{\sigma'}+\omega''_{\sigma''})\\ &-\frac{\boldsymbol{k}\boldsymbol{k}''+kk''}{kk''}\omega''_{\sigma''}(\omega''_{\sigma''}+\omega'_{\sigma'})+\frac{-\boldsymbol{k}'\boldsymbol{k}''+k'k''}{k'k''}\omega'_{\sigma'}\omega''_{\sigma''}+2(\omega')^2+2(\omega'')^2+2\omega'_{\sigma'}\omega''_{\sigma''}\Big]\\ &\times\alpha'_{\sigma'}\alpha''_{\sigma''}\epsilon^{\mathrm{i}(\omega_\sigma-\omega'_{\sigma'}-\omega''_{\sigma''})t}\Big\}\delta(\boldsymbol{k}-\boldsymbol{k}'-\boldsymbol{k}'')\,\mathrm{d}\boldsymbol{k}'\,\mathrm{d}\boldsymbol{k}''+O(\epsilon^2).\end{aligned} \tag{13}$$

The following abbreviations are used:

$$\left.\begin{aligned}&\omega=\omega(\boldsymbol{k}),\\ &\omega_\sigma=\begin{cases}\omega, & \sigma=1\\ -\omega, & \sigma=-1\end{cases},\quad \alpha_\sigma=\begin{cases}\alpha_+(\boldsymbol{k},t), & \sigma=1\\ \alpha_-(\boldsymbol{k},t), & \sigma=-1\end{cases}.\end{aligned}\right\} \tag{14}$$

In the summation σ' and σ'' take on the values -1 and $+1$, σ can be both $+1$ and -1.

Equation (13) governs the nonlinear interactions of water waves. One piece of information has not been used so far and should be added: the elevation and potential are real functions. This leads to a relation between α_+ and α_-. There are two conventions for stating this relation (Hasselmann 1962; Davidson 1972). I will have use for both of them here; the first convention is

$$\forall\boldsymbol{k}:\quad \alpha_+(\boldsymbol{k})=\alpha_-^*(-\boldsymbol{k}),\quad \omega_1=\omega,\quad \omega_{-1}=-\omega, \tag{15}$$

and the other

$$\left.\begin{aligned}&\forall k:\quad \sigma=-1,1;\quad \alpha_\sigma(\boldsymbol{k})=\alpha_\sigma^*(-\boldsymbol{k}),\quad \omega_\sigma(\boldsymbol{k})=-\omega_\sigma(-\boldsymbol{k}),\\ &\qquad\qquad k_x>0:\quad \omega_1=\omega,\quad \omega_{-1}=-\omega.\end{aligned}\right\} \tag{16}$$

The interactions described by (13) are cyclic in time except when the exponent vanishes, or, more explicitly, when

$$\boldsymbol{k}-\boldsymbol{k}'-\boldsymbol{k}''=0,\quad \omega_\sigma-\omega'_{\sigma'}-\omega''_{\sigma''}=0. \tag{17}$$

Waves fulfilling these conditions are called resonant waves. After a finite time the energy exchange between these waves will be far larger than between non-resonant waves. Note that resonant triads indeed exist for gravity–capillary waves (Simmons 1969) in contrast to the case of purely gravity waves (Hasselmann 1962; Zakharov 1968).

An equation similar to (13) has also been derived by Zakharov (1968) using not the Lagrangian but the Hamiltonian. Using, like Zakharov, the first version of the reality conditions I have checked that for resonant waves the equations are equal. For non-resonant waves the expressions are not equal. This is because only the resonant interactions are a true physical measurable phenomenon, therefore only these are independent of the representation (Henyey & Pomphrey 1982). Mathematically speaking there is uniform convergence for the resonant interactions but not for the non-resonant ones.

Simmons (1969) has derived a nonlinear interaction equation for the case of the surface elevation consisting of just three resonant waves. This can be considered as a special case of the present analysis; in this case the amplitudes of the modes are given by

$$\left.\begin{aligned}\alpha_+(\boldsymbol{k}) &= \pi \sum_{r=0}^{2} \alpha_r \delta(\boldsymbol{k}-\boldsymbol{k}_r),\\ \alpha_-(\boldsymbol{k}) &= \pi \sum_{r=0}^{2} \alpha_r^* \delta(\boldsymbol{k}+\boldsymbol{k}_r),\end{aligned}\right\} \tag{18}$$

where the wavevectors $\boldsymbol{k}_r$ satisfy the resonance conditions (17). I have checked that inserting (18) in (13) indeed regenerates the results of Simmons. The interaction coefficient in square brackets in (13) becomes equal for all of the three amplitudes. This identity will be used in §4.

Equation (13) describes the nonlinear interactions between gravity–capillary waves. However, as over a long time interval the non-resonant interactions do not contribute significantly to the exchange of energy between different waves (Longuet-Higgins & Smith 1966; McGoldrick *et al.* 1966), an evolution equation without these interactions is desirable. Such an equation can be derived both for the deterministic and for the stochastic case. The deterministic equation would be relevant for mechanically generated waves (Plant 1980) and the stochastic equation for wind waves. I only treat the stochastic case.

Here it is again important to note that the strength of the resonant interactions is a physical quantity independent of the representation. Therefore a renormalization of the system, consisting of transforming away the quadratic non-resonant modes (Meiss & Watson 1978; Guckenheimer & Holmes 1983, §3.3), will not affect the strength of this interaction (it will change the appearance of the interaction coefficient of course, just as any matrix looks different on a different base).

I assume that a nearly Gaussian distribution holds for the surface elevation (Hasselmann 1962). The following relations then hold for the cumulants or wave correlations ${}_nG$; α_σ is now the unscaled amplitude, cf. (5) and (7); also I use (16), the second version of the reality conditions:

$$\left.\begin{aligned}\langle \alpha_{\sigma_1}(\boldsymbol{k}_1)\,\alpha_{\sigma_2}(\boldsymbol{k}_2)\rangle &= G_{\sigma_1}(\boldsymbol{k}_1)\,\delta(\boldsymbol{k}_1+\boldsymbol{k}_2)\,\delta_{\sigma_1\sigma_2},\\ \langle \alpha_{\sigma_1}(\boldsymbol{k}_1)\,\alpha_{\sigma_2}(\boldsymbol{k}_2)\,\alpha_{\sigma_3}(\boldsymbol{k}_3)\rangle &= {}_3G_{\sigma_1\sigma_2\sigma_3}(\boldsymbol{k}_1,\boldsymbol{k}_2)\,\delta(\boldsymbol{k}_1+\boldsymbol{k}_2+\boldsymbol{k}_3),\\ \langle \alpha_{\sigma_1}(\boldsymbol{k}_1)\,\alpha_{\sigma_2}(\boldsymbol{k}_2)\,\alpha_{\sigma_3}(\boldsymbol{k}_3)\,\alpha_{\sigma_4}(\boldsymbol{k}_4)\rangle &= G_{\sigma_1}(\boldsymbol{k}_1)\,G_{\sigma_3}(\boldsymbol{k}_3)\,\delta(\boldsymbol{k}_1+\boldsymbol{k}_2)\,\delta(\boldsymbol{k}_3+\boldsymbol{k}_4)\,\delta_{\sigma_1\sigma_2}\delta_{\sigma_3\sigma_4}\\ &\quad + G_{\sigma_1}(\boldsymbol{k}_1)\,G_{\sigma_2}(\boldsymbol{k}_2)\,\delta(\boldsymbol{k}_1+\boldsymbol{k}_3)\,\delta(\boldsymbol{k}_2+\boldsymbol{k}_4)\,\delta_{\sigma_1\sigma_3}\delta_{\sigma_2\sigma_4}\\ &\quad + G_{\sigma_1}(\boldsymbol{k}_1)\,G_{\sigma_2}(\boldsymbol{k}_2)\,\delta(\boldsymbol{k}_1+\boldsymbol{k}_4)\,\delta(\boldsymbol{k}_2+\boldsymbol{k}_3)\,\delta_{\sigma_1\sigma_4}\delta_{\sigma_2\sigma_3}\\ &\quad + {}_4G_{\sigma_1\sigma_2\sigma_3\sigma_4}(\boldsymbol{k}_1,\boldsymbol{k}_2,\boldsymbol{k}_3)\,\delta(\boldsymbol{k}_1+\boldsymbol{k}_2+\boldsymbol{k}_3+\boldsymbol{k}_4).\end{aligned}\right\} \tag{19}$$

Here it is assumed, according to the near-Gaussian assumption, that each cumulant is small compared with the foregoing one. This assumption is crucial to the validity of weakly nonlinear theories; it will be checked in §6.

For the situation described by (19), Davidson (1972, chapter 13) gives a treatment of equations of the type (13). The use of two timescales and an ordering of the cumulants acording to $G \sim \epsilon$, ${}_nG \sim \epsilon^{n-1}$ are essential. Also, Davidson uses (16), the

second of the reality conditions. The result is a kinetic equation that describes the change in G_σ due to nonlinear interactions:

$$\frac{\partial}{\partial t}G_\sigma = \left\{\frac{k}{16\pi\omega_\sigma}\int\int J^2(\boldsymbol{k},\boldsymbol{k}',\boldsymbol{k}'')\,\delta(\boldsymbol{k}-\boldsymbol{k}'-\boldsymbol{k}'')\,\delta(\omega_\sigma-\omega'_\sigma-\omega''_\sigma)\right.$$
$$\left.\times\left[\frac{k}{\omega_\sigma}G'_\sigma G''_\sigma-\frac{k'}{\omega'_\sigma}G''_\sigma G_\sigma-\frac{k''}{\omega''_\sigma}G_\sigma G'_\sigma\right]\mathrm{d}\boldsymbol{k}'\,\mathrm{d}\boldsymbol{k}''\right\}(1+O(\epsilon)). \quad (20)$$

The interaction coefficient J is equal to that in square brackets of (13). For resonant triads, the only ones contributing to the right-hand side of (20), J can be simplified to

$$J(\boldsymbol{k}_0,\boldsymbol{k}_1,\boldsymbol{k}_2)=\sum_{p=0}^{2}\frac{\boldsymbol{k}_p\boldsymbol{k}_{p+1}-(-1)^p k_p k_{p+1}}{k_p k_{p+1}}\omega^p\omega^{p+1}. \quad (21)$$

The index $p+1$ should be interpreted modulo 3, and ω can have either sign. Equation (20) as written above is only valid under the second convention for stating the reality condition; thus $\omega_\sigma(\boldsymbol{k})=-\omega_\sigma(-\boldsymbol{k})$. Only under this convention does the summation over σ' and σ'' drop out of (20) and is the interaction coefficient J independent of σ, σ' and σ''. Physically the dropping out of the summation means that only waves travelling in the same direction can interact. This is caused by the frequency being a monotonously increasing function of wavenumber. The omission of higher-order corrections in the two-timescale expansion reduces the timescale on which (20) is valid to a scale of $1/\epsilon$. This is an order of magnitude larger than the timescale on which Valenzuela & Laing's results can formally be proved to be valid. Using a simple Poincaré-type expansion they obtain validity on a scale of 1.

The interaction equation (20) can be understood as follows. In the long run the change of the spectral density G_σ at certain wavenumber $\boldsymbol{k}$ is due only to interactions with those waves that satisfy the resonance conditions (17) in both frequency and wavenumber. Note that the Dirac delta functions in $\boldsymbol{k}$ and ω are equivalent to the set of equations (17). The interactions within the different resonant triads can be regarded as independent; thus the total change is the sum of the changes due to the various triads.

For each triad the strength of the interaction is proportional to the square of J. This J also appears as the interaction coefficient for the same resonant triad but in the discrete deterministic case as treated by Simmons (1969). One might say that the continuous stochastic result for the interactions follows from the discrete deterministic one by summing over all resonant triads and by squaring the interaction coefficient. However, in the discrete case the interaction is proportional to the product of the amplitudes of the two waves complemental to $\boldsymbol{k}$ within the triad while in the continuous case a combination of all three correlation functions appears.

To be able to check the assumption of near Gaussianity I also need an expression for the time development of the third cumulant. Note that near Gaussianity is defined by each cumulant being small compared with the foregoing one. Again following Davidson's (1972) work closely, this expression reads

$$\delta(\boldsymbol{k}_0-\boldsymbol{k}_1-\boldsymbol{k}_2)\,{}_3G_{\sigma_0\sigma_1\sigma_2}(\boldsymbol{k}_0,\boldsymbol{k}_1,t)=\frac{-\mathrm{i}}{4\pi}J(\boldsymbol{k}_0,\boldsymbol{k}_1,\boldsymbol{k}_2)\frac{\mathrm{e}^{\mathrm{i}t(\sigma_0\omega_0-\sigma_1\omega_1-\sigma_2\omega_2)}-1}{\mathrm{i}(\sigma_0\omega_0-\sigma_1\omega_1-\sigma_2\omega_2)}$$
$$\times\left[\frac{k_0}{\omega_{0\,\sigma_0}}G_{\sigma_1}(\boldsymbol{k}_1)\,G_{\sigma_2}(\boldsymbol{k}_2)-\frac{k_1}{\omega_{1\,\sigma_1}}G_{\sigma_2}(\boldsymbol{k}_2)\,G_{\sigma_0}(\boldsymbol{k}_0)\right.$$
$$\left.-\frac{k_2}{\omega_{2\,\sigma_2}}G_{\sigma_0}(\boldsymbol{k}_0)\,G_{\sigma_1}(\boldsymbol{k}_1)\right]\delta(\boldsymbol{k}_0-\boldsymbol{k}_1-\boldsymbol{k}_2)+{}_3G_{\sigma_0\sigma_1\sigma_2}(\boldsymbol{k}_0,\boldsymbol{k}_1,0). \quad (22)$$

Equation (22) shows immediately that for non-resonant waves $\boldsymbol{k}_0, \boldsymbol{k}_1$ the third cumulant oscillates rapidly. Therefore it is only at resonant triads that the third cumulant is of interest. Comparing (20) and (22) shows that at resonant triads the integrand of (20) is proportional to the third cumulant minus its initial value. This is in accordance with the fact that no nonlinear transfer occurs in a Gaussian sea.

Davidson (1972) has shown in general by entropy arguments that under influence of triad interactions $G_\sigma(\boldsymbol{k})$ goes to a function for which the nonlinear transfer is zero:

$$\frac{k_0}{\omega_{0\sigma_0} G_{\sigma_0}(\boldsymbol{k}_0)} = \frac{k_1}{\omega_{1\sigma_1} G_{\sigma_1}(\boldsymbol{k}_1)} + \frac{k_2}{\omega_{2\sigma_2} G_{\sigma_2}(\boldsymbol{k}_2)}, \tag{23}$$

for all waves fulfilling

$$\omega_0 = \omega_1 + \omega_2, \quad \boldsymbol{k}_0 = \boldsymbol{k}_1 + \boldsymbol{k}_2. \tag{24}$$

Using the relation between the third cumulant and the transfer this implies that the third cumulant goes to a constant. In §6 it will be checked that this result still holds for an energy balance that contains linear as well as nonlinear terms.

A few more remarks concerning the interaction are relevant. First, the spectral densities G_σ are closely related to the energy E:

$$\left.\begin{aligned} E_{\text{tot}} &= \int\int_{-\infty}^{+\infty} E(\boldsymbol{k})\,\mathrm{d}\boldsymbol{k}, \\ E(\boldsymbol{k}) &= \frac{\rho\omega^2}{\pi^2 k}[G_+(\boldsymbol{k}) + G_-(\boldsymbol{k})]. \end{aligned}\right\} \tag{25}$$

Kinetic equations like (20), based on equations of the type (13), occur in many fields of physics, for instance plasma physics (Davidson 1972). The expression for the interaction coefficient is specific to the problem at hand. It can be easily proved that equations of the type (20) guarantee conservation of energy and momentum (Davidson 1972, p. 254). Also, as

$$\lim_{k \downarrow 0} \frac{k}{\omega(\boldsymbol{k})} J(\boldsymbol{k}, \boldsymbol{k}', -\boldsymbol{k}') = 0,$$

the mean surface elevation remains zero for all times (Davidson 1972, p. 247). The scaling of the interactions follows directly from (20): when all the energies are multiplied by a constant factor λ the interaction time T_{NL} defined by $E/(\partial E/\partial t)$ is reduced by a factor λ:

$$\left(E \Big/ \frac{\partial E}{\partial t}\right)\Big|_{E=\lambda E_0} = \frac{1}{\lambda}\left(E \Big/ \frac{\partial E}{\partial t}\right)\Big|_{E=E_0}. \tag{26}$$

Finally, (20) is formally invalid at $k = (2g/T)^{\frac{1}{2}}$; that is at the wavenumber for which second harmonic resonance occurs. At this wavenumber a singularity arises in the transfer. However, the singularity is integrable and the energy spectrum itself remains finite (see §6).

The present expression (20) for the energy transfer due to nonlinear interactions can be shown to be equal to that presented by Krasil'nikov & Pavlov (1973). The expression of Valenzuela & Laing (1972), when corrected for misprints as noticed by Holliday (1977), is equal to the aforementioned two except that it is a factor 2 smaller. This difference was noted by Plant (1979).

3. Multiwave space

As an introduction to multiwave space I want to show how I went about ascertaining that I would find all resonant waves when I started this study. Here and in the following sections the analysis is restricted to parallel waves. The structure of the division of the resonant triads over wavenumber space depends only on the dispersion relation. Simmons (1969) has presented graphical methods to find the triads. I present here as figure 1 his figure showing the construction of a resonant triad. Table 1 shows several such triads. From figure 1 the following structure can be obtained. For a relatively long wave, almost in the gravity region, just one triad exists. Such a wave interacts with two very short waves of nearly equal wavenumber in the extreme capillary region. If the first wavenumber becomes larger, the two resonant wavenumbers decrease and move further apart. When the first wavenumber approaches $\frac{1}{2}k_0$, where k_0 is defined by

$$k_0 = (2g/T)^{\frac{1}{2}}, \tag{27}$$

the intermediate wavenumber approaches this same value from above and the largest wavenumber drops to k_0, as illustrated by table 1 and figures 1 and 2. In the case where the shortest wavenumber equals $\frac{1}{2}k_0$ the intermediate and the shortest wavenumber are equal and can no longer be distinguished. This is the situation called second-harmonic resonance. If the first wavenumber is allowed to grow even further it is clear that the triads already found will be re-encountered, the 'basic' wave being now the intermediate wave of a triad. A second triad for the 'basic' wave appears when k becomes larger than k_0. The 'basic' wave is then the intermediate wave of one triad and the wave with largest wavenumber of the other triad.

The description above implies the following: all resonant triads between gravity–capillary waves are encountered once and just once when a triad is calculated for each wave out of the set

$$0 \leqslant k \leqslant \tfrac{1}{2}k_0. \tag{28}$$

A formal proof of this statement is now given.

Resonant triads are defined by (cf. (16) and (17) and the discussion below (21)):

$$\boldsymbol{k}-\boldsymbol{k}'-\boldsymbol{k}'' = 0, \quad \omega_\sigma-\omega'_\sigma-\omega''_\sigma = 0, \quad \omega_\sigma(-\boldsymbol{k}) = -\omega_\sigma(\boldsymbol{k}).$$

Note, again, that different modes do not interact. In the following I choose one mode, the reasoning is exactly the same for the other. The resonance conditions generate two sets of solutions:

$$\left.\begin{aligned} &\text{sum triads:} && \boldsymbol{k}-\boldsymbol{k}_s-\boldsymbol{k}_m = 0, \\ &&& \omega-\omega_s-\omega_m = 0 \quad (\forall k, \omega(\boldsymbol{k}) > 0), \\ &\text{difference triads:} && \boldsymbol{k}+\boldsymbol{k}_q-\boldsymbol{k}_p = 0, \\ &&& \omega+\omega_q-\omega_p = 0 \quad (\forall k, \omega(\boldsymbol{k}) > 0). \end{aligned}\right\} \tag{29}$$

For each set all wavevectors lie in one half of the plane; a direct consequence of the non-interaction of different modes. One-dimensionally the wavevector can thus be substituted by its length. In the one-dimensional case the sum and difference triads are each defined by two equations for three unknowns. Thus for given k they each generate at most one solution. For every k a solution to the minus triad can be found; this follows trivially from figure 1. The sum triad only exists for $k \geqslant k_0$ (Simmons 1969). This already proves part of the statement, i.e. that for $k \leqslant \frac{1}{2}k_0$ exactly one resonant triad exists. The other part of the statement is that no new triads can be found once a triad for each $k \leqslant \frac{1}{2}k_0$ has been constructed. This comes about as follows.

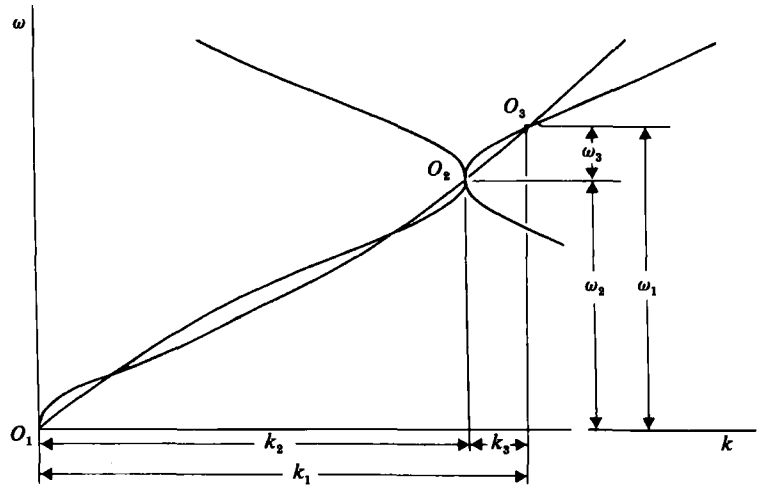

FIGURE 1. Graphical construction of resonant triads in the one-dimensional case. The dispersion relation $\omega(k)$ is plotted with O_1 as origin. To find the resonant wavenumbers for k_2 it is again plotted with O_2 as origin. Intersection points between the two graphs determine resonant triads; the wavenumbers are given by the horizontal distances between the intersection point and O_1 and O_2 respectively. From Simmons (1969).

k (m^{-1})	k_m (m^{-1})	k_l (m^{-1})
48.0	1280.9	1328.9
53.8	1149.0	1202.8
60.2	1031.5	1091.7
67.4	926.7	994.1
75.5	833.1	908.7
84.6	749.6	834.2
94.7	674.8	769.5
106.1	607.6	713.8
118.8	547.3	666.2
133.1	492.9	626.0
149.1	443.7	592.8
167.0	399.1	566.1
187.0	358.5	545.6
209.4	321.7	531.1
234.6	288.0	522.6

TABLE 1. The resonant wavenumbers k_m and k_l as a function of k; an example of the type of grid used for numerical calculations (k, k_m and k_l being the grid points)

A sum triad for any k is identical with the difference triads for both $k_s(k)$ and $k_m(k)$. Thus the sum triads give no new solutions. Next, in any difference triad for $k > \frac{1}{2}k_0$, $k_q < \frac{1}{2}k_0$ holds, see Appendix A; thus indeed $k > \frac{1}{2}k_0$ gives no new triads. The last part of the statement to check is that two triads for different k, both satisfying $k < k_0$, cannot be identical. This follows from the fact that for any $k < \frac{1}{2}k_0$, $k_q > \frac{1}{2}k_0$ (Simmons 1969).

Note that a by result of the above proof is that the sum and difference sets of solutions are equal. The difference between the conditions is not their total solution, thus not the triad, but the role k has in the triad. For a sum triad k is the largest

wavenumber while for a difference triad k is the smallest or intermediate wavenumber.

All the foregoing information, and more, can be brought together in one graph, in the multiplet–wavenumber space. The dimension M of the multiplet space is the dimension of the space of a branch of solutions to the resonance conditions. Thus for one- or two-dimensional triad interactions it is respectively one or three; for quadruplet interactions it is respectively two or five. As coordinates $(m_1, \ldots, m_M)$ in this space I have chosen M components of wavevectors. These identify the multiplet completely. By systematically choosing these M components from the smallest wavevectors each multiplet has a unique representation. In the present case I have taken $m = k_s$. Multiwave space is the direct product of multiplet and wavevector space.

In two-dimensional triad-wavenumber space the solutions to the resonance conditions can be represented by

$$\left.\begin{aligned} &x = (k, m), \quad m = m(k) = -c_1 \log\left(\frac{k_s}{c_2}\right), \quad k_s \leqslant k_m < k_l, \\ &k_s + k_m - k_l = 0, \quad \omega_s + \omega_m - \omega_l = 0, \quad k \in \{k_s, k_m, k_l\}, \end{aligned}\right\} \tag{30}$$

The function $m(k_s)$ has been chosen for convenience. This mapping has been drawn in figure 2; the scale for m is arbitrary. For $k < k_0$, $m(k)$ is single-valued, for $k \geqslant k_0$ double-valued. This bifurcation point plays an important role in the following analysis.

Multiwave space can be used to find the resonant wavenumbers for a given wavenumber k^0. This is done by searching for other wavenumbers for which (30) defines the same m, in other words, by searching for cross-points between $m(k^0)$ and the horizontal line through $m(k^0)$. These wavenumbers will be called $k^1(k^0)$.

This process can be continued, for the set $\{k^1(k^0)\}$ a resonant set $\{k^2(k^0)\}$ can be found, etc. This is done by drawing horizontal and vertical lines from $(k^i, m(k^i))$. For definiteness elements k^{i-1} will not be considered part of $\{k^i\}$. The union of these sets will be called $K(k^0)$. Within a set $K(k^0)$ all waves exchange energy. If there are waves $k \notin K(k^0)$ these develop independently of this set. This makes it important, both to understanding nonlinear interactions and to performing accurate numerical calculations, to find how these sets cover wavenumber space.

To find this I restrict myself to a finite, though arbitrarily wide, interval of wavenumbers:

$$k \in [k_{\min}, k_{\max}],$$

where for convenience $k_{\max}$ and $k_{\min}$ are resonant and $k_{\max}$ is chosen such that

$$\exists n \in \mathbb{N}: \quad k \in \{k^n(k_0)\}.$$

As an illustration of this point part of the set $K(k_0)$ is drawn in figure 2. The following division of wavenumber space exists: consider

$$A = (\tfrac{1}{2}k_0, k_0],$$

$$K(k^0) = \bigcup_{i=0}^{n} \{k^i(k^0)\}.$$

THEOREM 1. *For $k_a, k_b \in A$ $K(k_a) \cap K(k_b) = \varnothing$ unless $k_a = k_b$.*

THEOREM 2. $\bigcup_{k^0 \in A} K(k^0) = [k_{\min}, k_{\max}]$.

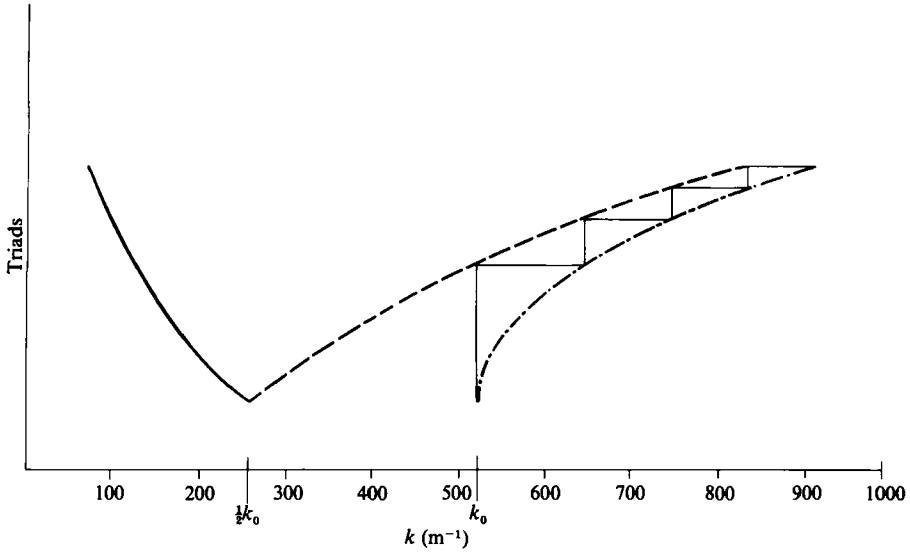

FIGURE 2. The resonant wavenumbers k_m and k_l as a function of k, see table 1. Different triads are indicated by different heights. Note that for $k > k_0$ every wave participates in two triads, for $k < \frac{1}{2}k_0$, k is the smallest wavenumber of a triad. ——, Smallest wavenumber of a triad k; – – – –, intermediate wavenumber of a triad k_m; –·–·–, largest wavenumber of a triad k_l.

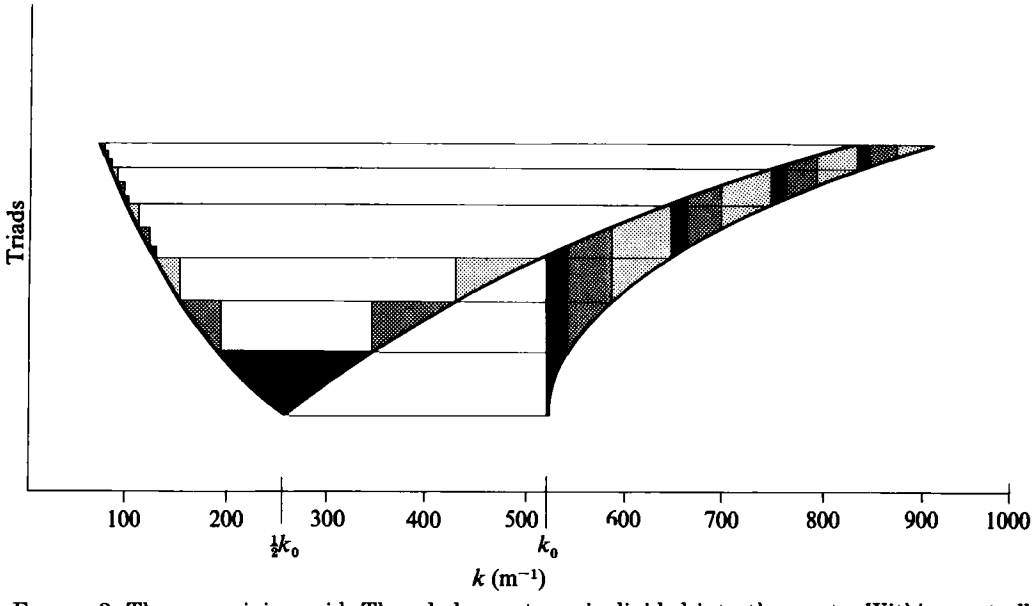

FIGURE 3. The non-mixing grid. The whole spectrum is divided into three sets. Within a set all waves are coupled, but the sets develop independently of each other. A division of the interval $(\frac{1}{2}k_0, k_0]$ in R sets, represented by k_r, generates R independent sets represented by $K(k_r)$.

$$\bigcup_{k^0 \in (\frac{1}{2}k_0,\ \frac{2}{3}k_0]} K(k^0)$$

$$\bigcup_{k^0 \in (\frac{2}{3}k_0,\ \frac{5}{6}k_0]} K(k^0)$$

$$\bigcup_{k^0 \in (\frac{5}{6}k_0,\ k_0]} K(k^0)$$

Thus there exist infinitely many independent sets. Each set is uniquely represented by a wavenumber k^0 in the interval $\frac{1}{2}k_0 < k^0 \leqslant k_0$. Proofs of theorems 1 and 2 are given in Appendix B.

If one divides the interval between $\frac{1}{2}k_0$ and k_0 into, for instance, three finite regions this will generate three independent sets, together covering the whole wavenumber axis. This has been plotted in figure 3. By using the intervals so constructed as bins (the bands Δk_i around the representatives k_i in a discretization of the wavenumber axis) in a numerical model the independence of these sets is maintained. Any other choice of bins would implicitly lay a link between the sets. Both options will be used in §§5 and 6; it will be seen that this choice has important consequences.

Multiwave space also makes possible estimates of the magnitude of the transfer of energy without doing any calculations. The transfer is roughly proportional to the slope $\partial m/\partial k$. This proportionality is a direct result of the fact that, instantaneously, the total energy transfer is zero in a horizontal band Δm of arbitrary width. This will be shown in the next paragraph. From the relation between transfer and slope combined with figure 2 it can be inferred that at k_0 the transfer has a singularity. The energy at k_0 will rise quickly until the integrand of (20), i.e. the third cumulant, is zero at this point. The energy level of other members of $K(k_0)$ will also be affected. Thus one expects to see peaks in the spectrum at $k \in K(k_0), k \geqslant k_0$ and dips at $k \in K(k_0), k < k_0$ (for the sign of the transfer I use results of the next sections). When an equilibrium is reached these dips and peaks will have disappeared again, because the equilibrium is smooth (cf. (23)).

To prove that the total energy transfer is zero in a band $[m_1, m_2]$ only the $\sigma = +1$ mode need be considered. Then the following relation holds:

$$\int_{m_1}^{m_2} \frac{\partial E}{\partial t}\,\mathrm{d}m = \int_{m_1}^{m_2} \sum_{i=0}^{2} \frac{\rho\omega_i^2}{\pi^2 k_1} \frac{\partial G(m)}{\partial t}\,\mathrm{d}m$$

$$= \frac{\rho}{\pi^2} \sum_{i=0}^{2} \int_{k_i(m_1)}^{k_i(m_2)} \frac{\omega_i^2}{k_i} \left[\frac{\partial G(k_i)}{\partial t}\right]^* \mathrm{d}k. \tag{31}$$

The asterisk indicates that only those contributions should be considered for which $m(k_s) \in [m_1, m_2]$, k_s being the smallest resonant wavenumber. Using (20) gives

$$\int_{m_1}^{m_2} \frac{\partial E}{\partial t}\,\mathrm{d}m = \frac{\rho}{16\pi^3} \sum_{i=0}^{2} \int_{k_i(m_1)}^{k_i(m_2)} \int_{-\infty}^{+\infty} \int_{-\infty}^{+\infty} \omega_i J^2(k_i, k', k'')\,\delta^*(k_i - k' - k'')$$

$$\times\, \delta^*(\omega_i - \omega' - \omega'') \left[\frac{k_i}{\omega_i} G' G'' - \frac{k'}{\omega'} G'' G_i - \frac{k''}{\omega''} G_i G'\right] \mathrm{d}k'\,\mathrm{d}k''\,\mathrm{d}k_i.$$

Definition (30) states, among other things, that if $k_i - k_p - k_q = 0$ and $\omega_i - \omega_p - \omega_q = 0$ then $m(k_p) = m(k_q) = m(k_i)$. Therefore the integration boundaries can be substituted as follows:

$$\int_{m_1}^{m_2} \frac{\partial E}{\partial t}\,\mathrm{d}m = \frac{\rho}{16\pi^3} \sum_{i=0}^{2} \int_{k_i(m_1)}^{k_i(m_2)} \int_{k_p(m_1)}^{k_p(m_2)} \int_{k_q(m_1)}^{k_q(m_2)} \omega_i J^2(k_i, k', k'')$$

$$\times\, \delta^*(k_i - k' - k'')\,\delta^*(\omega_i - \omega' - \omega'') \left[\frac{k_i}{\omega_i} G' G'' - \frac{k'}{\omega'} G'' G_i - \frac{k''}{\omega''} G_i G'\right] \mathrm{d}k'\,\mathrm{d}k''\,\mathrm{d}k_i.$$

The rest of the argument follows Davidson's (1972) proof for the conservation of the total energy. Interchanging integration variables k_i, $-k'$ and $-k''$ and relabelling the k's gives

$$\int_{m_1}^{m_2} \frac{\partial E}{\partial t}\,\mathrm{d}m = \frac{1}{3}\frac{\rho}{16\pi^3}\sum_{i=0}^{2}\int_{k_s(m_1)}^{k_s(m_2)}\int_{k_m(m_1)}^{k_m(m_2)}\int_{k_l(m_1)}^{k_l(m_2)} (\omega_l-\omega_s-\omega_m)$$
$$\times J^2(k_l,k_s,k_m)\,\delta^*(k_l-k_s-k_m)\,\delta^*(\omega_l-\omega_s-\omega_m)$$
$$\times\left[\frac{k_1}{\omega_1}G_s G_m-\frac{k_s}{\omega_s}G_m G_l-\frac{k_m}{\omega_m}G_l G_s\right]\mathrm{d}k_l\,\mathrm{d}k_m\,\mathrm{d}k_s,$$

where use of the symmetries of J has been made (see next section). Because $\omega_l-\omega_s-\omega_m$ equals zero for all solutions to the Dirac delta functions this gives

$$\int_{m_1}^{m_2}\frac{\partial E}{\partial t}\,\mathrm{d}m = 0, \tag{32}$$

i.e. the total transfer in a band $[m_1, m_2]$ is zero. Note that this result only holds instantaneously; in a finite time interval the transfers from the two triads for $k \geqslant k_0$ add up and energy conservation, for each band Δm separately, is destroyed. In §5, (32) will be used to construct a numerical grid that guarantees high accuracy.

4. Symmetries within the triads

The transfer of energy from one choice of two waves out of a triad to the third member is simply related to that of any other choice of two waves out of the same triad to a third member. This type of symmetry in the transfer equations is related to weakly nonlinear interactions in general; any three-wave interaction process would exhibit it. The following is essential. If k_s, k_m, k_l form a resonant triad, according to $k_l-k_s-k_m=0$, then

$$J(k_l,k_s,k_m) = J(k_s,-k_m,k_l) = J(k_m,k_l,-k_s), \tag{33}$$

and defining

$$R_\sigma(k;k'k'') = \frac{k}{\omega_\sigma}G'_\sigma G''_\sigma - \frac{k'}{\omega'_\sigma}G''_\sigma G_\sigma - \frac{k''}{\omega''_\sigma}G_\sigma G'_\sigma$$

we also have

$$R_\sigma(k_l;k_s,k_m) = -R_\sigma(k_s;-k_m,k_l) = -R_\sigma(k_m;k_l,-k_s). \tag{34}$$

Thus in one dimension the set of transfer equations (20) can be simplified to the following:

$$\left.\begin{aligned} k = k_{is}, k_{im} \quad &\text{or } k_{il}, k_{il}-k_{is}-k_{im}=0,\\ \omega_{il}-\omega_{is}-\omega_{im} &= 0,\\ \frac{\partial}{\partial t}G_\sigma(k) = \frac{k}{8\pi\omega_\sigma}\sum_{i=1}^{2} &\, s J_i^2(k)\,R_\sigma(k_{il};k_{is},k_{lm})\,|c_{g\sigma}(k_{ip})-c_{g\sigma}(k_{iq})|^{-1}, \end{aligned}\right\} \tag{35}$$

$$J_i(k) = 2|\omega_\sigma(k_{is})\,\omega_\sigma(k_{im})|. \tag{36}$$

If $k = k_{is}, k_{im}$ then $s = 1$,

If $k = k_{il}$ then $s = -1$.

Here k, k_{ip} and k_{iq} form a resonant triad and c_g is the group velocity: $c_{g\sigma} = \partial\omega_\sigma/\partial k$. The summation over $i = 1, 2$ reflects the existence of sum and difference triads. Note that J_i has been simplified.

5. Discretization

The kinetic equation (20) is not in general solvable analytically. Whether it can be solved depends on the solutions to the resonance conditions. Davidson (1972, pp. 258–260) gives a solution for the one-dimensional case in which each wave only participates in exactly one triad. Simmons (1969) and McGoldrick (1970) have treated the case of just one resonant triad. I do not attempt to give an analytical solution here; I present efficient methods to determine the value of the nonlinear interactions for a given spectrum. In the next section the spectrum will be integrated using these methods.

The methods presented here are efficient because they use natural grids, to be introduced below, and the symmetries of the integrand shown in §4. These methods are more accurate than previous ones. Also, they do not require recalculation of the same factors. At the same accuracy the present methods are estimated to be more than an order of magnitude quicker than the straightforward ones: a factor 3 for doing calculations once per triad, using (35), a factor 2 for not treating sum and difference triads separately, and at least a factor 2 for higher accuracy at the same bandwidth.

The fact that the net transfer in a band Δm is zero can be used in a numerical model to guarantee energy conservation for the whole spectrum. This is done by choosing gridpoints on the wavenumber axis as follows. The triad axis is discretized arbitrarily into a set m_j with bins Δm_j. The gridpoints and bins in wavenumber space I choose as

$$\left.\begin{aligned} k_{ij} &= k_i(m_j), \\ \Delta k_{ij} &= k_i(m_j+\tfrac{1}{2}\Delta m_j)-k_i(m_j-\tfrac{1}{2}\Delta m_j), \end{aligned}\right\} \tag{37}$$

where i ranges over the three members of a triad. Equation (37) implies that all gridpoints exactly resonate with two other points. Within such a triad the net transfer is zero by (32). The transfer being zero per triad helps to guarantee conservation of total energy in a numerical model. I call grids given by (37) natural, because they follow directly from the structure of the resonant triads.

In this study two natural grids are used. The first one has the sets $K(\frac{7}{12}k_0)$, $K(\frac{9}{12}k_0)$ and $K(\frac{11}{12}k_0)$ as gridpoints. The boundaries of the bins are given by $K(\frac{8}{12}k_0)$, $K(\frac{10}{12}k_0)$ and $K(k_0)$. This grid is shown in figure 3. On this grid no mixing occurs between the independent sets found in §3. This grid will be called the non-mixing grid. With 33 triads the total energy is conserved with an accuracy $(\Delta E_{\mathrm{tot}}/E_{\mathrm{tot}})/(\Delta G_+(k)/G_+(k)) \approx 10^{-9}$.

The second grid is based on bands Δm_j of constant width (under the mapping $m(k) = -c_1 \log(k_s/c_2)$). A complexity that arises here is that, because $m(k)$ is double-valued for $k \geqslant k_0$, there are two grids for $k \geqslant k_0$. They consist of wavenumbers that are respectively the intermediate and the largest members of triads, a k_m and k_l grid (note that for the non-mixing grid these two coalesce). What is being done here is that the two contributions to the transfer in (35) are each calculated on a separate grid. The two have to be added to determine the total transfer. The addition is performed on the k_m grid after linearly interpolating the transfers on the k_l grid to the k_m grid. Before the next integration step can be performed the spectrum G_+ has to be interpolated back to the k_l grid. This is done by taking $G_+(k_m)$, for k_l in the band around k_m. At k_0 a peak arises in the transfer (see Valenzuela & Laing 1972 or §6), therefore the interpolation in the neighbourhood of k_0 has to be performed

with more care. In the k_m band containing k_0 analytical considerations on the shape of the transfer peak lead me to take

$$G_+(k_l) = \max\left\{\hat{G}_+(k_l), \min\left(G_+(k_{m+1})\frac{k_{m+1}-k_0}{k_l-k_0}, \frac{G_+(\frac{1}{2}k_0-\Delta)\,G_+(\frac{1}{2}k_0+\Delta)}{G_+(\frac{1}{2}k_0-\Delta)+G_+(\frac{1}{2}k_0+\Delta)}\right)\right\}. \quad (38)$$

Here k_{m+1} is the grid point on the k_m band next to the band containing k_0, $\hat{G}_+$ is the spectral level determined by linear interpolation and $\frac{1}{2}k_0-\Delta$ and $\frac{1}{2}k_0+\Delta$ are respectively the nearest members to $\frac{1}{2}k_0$ on the k_s and k_m grid. On this second grid a loss of accuracy occurs because of the interpolation to and forth. Still, with 35 triads the accuracy is given by $(\Delta E_{\text{tot}}/E_{\text{tot}})/(\Delta G_+(k)/G_+(k)) \approx 10^{-2}$. An important difference with the first grid is that on this one the sets K are no longer independent. As an illustration of this consider the following. The four lowest horizontal bands in figure 3, more or less of equal width, can be thought of as generating a wavenumber grid of the second type. The highest band of the four contains all sets K, thereby mixing them all. This mixing will be seen in §6 to have far-reaching consequences.

For the integration a first-order forward scheme is used. As a check a leapfrog scheme has been used; this gave the same results. At the high-wavenumber boundary a tail with adjustable power and coefficient has been fitted. The wavenumber interval is chosen by keeping in mind that viscosity has not been incorporated in the present theory. The expressions only make sense, therefore, when viscous damping acts on the same or a larger timescale as the nonlinear interactions (assuming the strength of the coupling of the two effects to be roughly equal to the product of the strength of the two effects). I have chosen $k_{\max} \approx 1300\ \text{m}^{-1}$ in accordance with Valenzuela & Laing (1972) who take

$$k_{\max} = (3-4)\,(g/2T)^{\frac{1}{2}} \approx 1100-1500\ \text{m}^{-1}.$$

The timescales of the two effects at this boundary will be explicitly compared in §6. As the longest wave resonates with the shortest this immediately gives $k_{\min} \approx 50\ \text{m}^{-1}$.

6. Spectral development

The nonlinear interactions have been calculated for various spectra. Figure 4 shows the transfer for a spectrum measured by Liu & Lin (1982) in a wave tank for a windspeed of 7 m/s. This result is typical for any smooth spectrum with a peak at low wavenumbers. Actually, I have approximated the spectrum of Liu & Lin. An explicit description of the spectrum in SI units reads:

$$\left.\begin{aligned}
\tilde{G}_+(\nu) &= 16.8\pi^2\,10^{-6}\left(\frac{\nu}{4.2}\right)^{6}, \qquad (\nu \leqslant 4.2)\\
\tilde{G}_+(\nu) &= 16.8\pi^2\,10^{-6}\left(\frac{\nu}{4.2}\right)^{-5.1}, \quad (4.2 \leqslant \nu \leqslant 15)\\
\tilde{G}_+(\nu) &= 25.6\pi^2\,10^{-9}\left(\frac{\nu}{15}\right)^{-2.5}, \quad (15 \leqslant \nu)\\
\nu &= \frac{\omega(k)}{2\pi}, \quad G_+(k) = \frac{c_g}{4\pi}\tilde{G}_+(\nu).
\end{aligned}\right\} \quad (39)$$

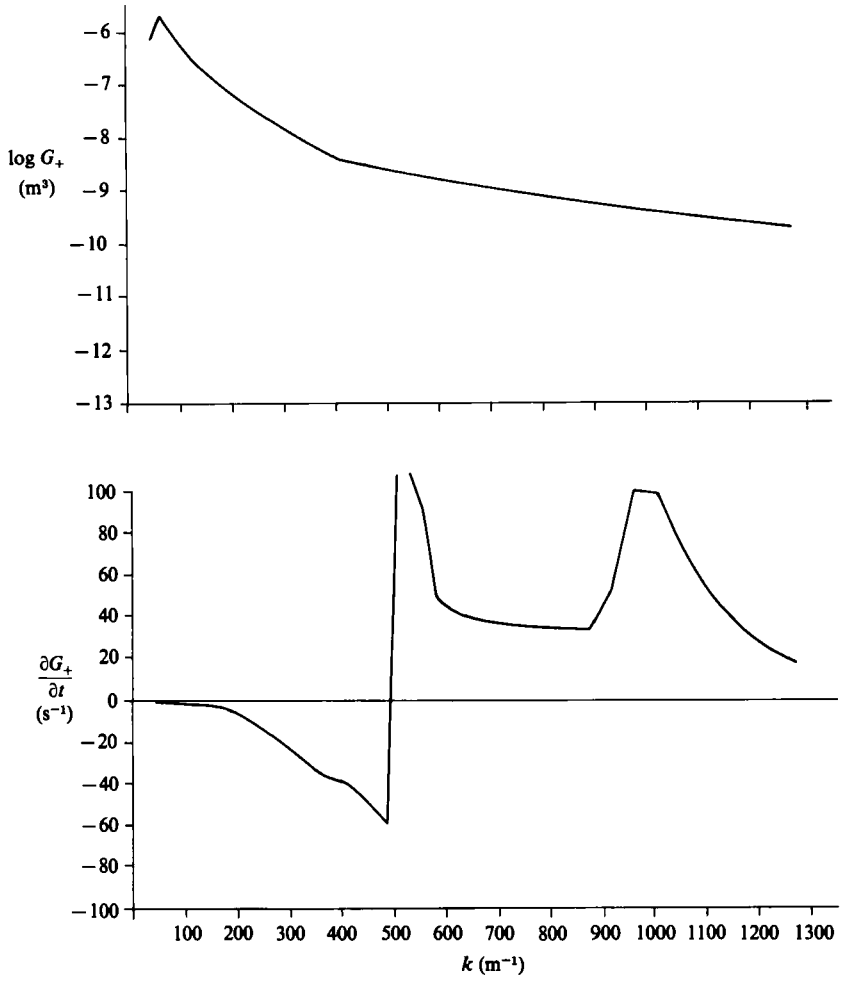

FIGURE 4. Variance spectrum G_+ and transfer $\partial G_+/\partial t$. The spectrum follows closely the measurements of Liu and Lin (1982) for a windspeed of 7 m/s.

Here (25) gives the relation between G_σ and the energy E; G_- equals zero, $\tilde{G}_+(\nu)$ is divided equally over k and $-k$ and the tilde is used to indicate the dependence on the frequency ν.

In principle the sign of the transfer at a given wavenumber can be positive or negative, depending on the energy level at all members of the triads resonant for this wavenumber. However, for any spectrum somewhat like k^{-n} the general tendencies are the same. Energy flows away from the peak of the spectrum towards wavenumbers larger than k_0; numerically $k_0 = 520.11$ m^{-1}. The main transfer is to the region close to k_0, roughly between 520 and 620 m^{-1}. This is in accordance with the prediction at the end of §3. For the transfer the results are indistinguishable for the two grids.

Nonlinear interactions for this type of spectrum have also been shown by Valenzuela & Laing (1972). What is new in figure 4 is that measured spectra are now available. The height of the spectrum is important as this determines the strength of the nonlinear interactions. For the first time a comparison can be made between

u_* (m/s)	k (m^{-1})	T_w (s)	T_{NL} (s)
0.21	200	0.8	0.3
	300	0.6	0.1
	450	0.5	0.06
	540	0.7	0.01
	600	0.8	0.03
	800	∞	± 1
0.35	200	0.91	0.2
	300	0.16	0.06
	450	0.14	0.03
	540	0.14	0.01
	600	0.13	0.03
	800	0.14	0.04
0.5	200	—	0.1
	300	—	0.03
	450	0.04	0.01
	540	0.05	0.005
	600	0.05	0.01
	800	0.05	0.03

TABLE 2. Comparison of the timescales T_w and T_{NL}, respectively for growth due to the wind and for nonlinear interactions, as a function of wavenumber for various windspeeds

the timescale of the growth of the waves due to the wind, the positive source term in the energy balance (1) for gravity–capillary waves, and that of the nonlinear interactions. I use the method of van Gastel *et al.* (1985) to determine this timescale. In this method viscosity is taken into account, so actually a net source term, which is approximated by the sum of S_w and S_{visc}, is compared to the nonlinear interactions. van Gastel *et al.* use u_*, the friction velocity, to characterize the wind speed, while the measurements are for given U. I use here the rule of thumb $u_* = \frac{1}{20}U$ to relate U and u_*. Typical timescales T_w of $S_w + S_{visc}$ and T_{NL} can be found in table 2. Not all of the spectrum used in this paper, i.e. 48 m$^{-1} \leqslant k \leqslant 1300$ m^{-1}, is covered by these data, but the middle part, where the interesting dynamics occur, is. For this region T_{NL} is smaller than T_w at every wavenumber for all wind speeds; thus the nonlinear interactions have more effect on the energy level of the waves than the wind. Near the peak of the nonlinear transfer an order-of-magnitude difference exists between the two effects, far from the peak the effects are nearly equal.

In choosing the cutoff wavenumber for the calculations it has been assumed that throughout the interval the timescale of the viscous damping T_ν is at least as large as T_{NL}, T_{NL} being the timescale of nonlinear interactions defined above (24). T_ν is equal to $(4\nu k^2)^{-1}$, ν being the kinematic viscosity (Phillips 1977, p. 52). This condition is fulfilled throughout the whole interval for the present case; that is $U = 7$ m/s. In this case for all wavenumbers $T_\nu/T_{NL} \geqslant 3$. However, for a realistic spectrum at $U = 4$ m/s a new cutoff wavenumber has to be chosen at $k = 800$ m^{-1}, implying a minimum wavenumber of 90 m^{-1}.

What has not appeared before in the literature is the integration of an energy balance including nonlinear interactions. I have done this for the case of gravity–capillary 'swell', that is I have studied the fetch development for realistic initial states in case only nonlinear interactions and viscous damping act. Wind, current and

breaking are absent in this case. In a follow-up study (van Gastel 1987), these effects are included. Thus the equation that has been integrated is

$$\frac{\partial G_+}{\partial x} = \frac{1}{c_g}[S_{nl} - 4\,\nu k^2\, G_+], \tag{40}$$

where S_{nl} is given by (20) or, equivalently, by (35).

Figures 5 and 6 show the fetch development of gravity–capillary swell. The integration is performed on the mixing grid. Initial spectra were measured by Liu & Lin (1982), for windspeeds of 7 and 4 m/s respectively. The spectrum at 4 m/s is approximated in a manner similar to that used at 7 m/s (see (39)). It is seen that the peak in the transfer at k_0, evident in figure 4, does not result in singular behaviour of the energy density. For the case of a low wind speed a finite peak appears at k_0; for the high-wind-speed case the spectrum is almost smooth. This is because at low wind speeds the nonlinear interactions are relatively smaller, thus they are more thwarted in trying to reach an equilibrium (see the top paragraph on p. 511). Indeed, for $U = 7$ m/s the tail of the spectrum ($k = 300$–1100 m^{-1}) has the equilibrium shape of (23).

It is seen that, also in accordance with the predictions of §3, the whole set $K(k_0)$ is affected by the transfer peak at k_0. There are dips for $k \in K(k_0), k < k_0$ and peaks for $k \in K(k_0), k \geqslant k_0$. The wavenumbers of these peaks all follow from figure 2. The first four are given by

$$k = 520, 646, 745, 830 \text{ m}^{-1}. \tag{41}$$

Translated into the appearance of the surface, these peaks mean that there are preferred wavelengths. Some wavelengths will be seen more often to dominate the appearance of the surface than others. The four most preferred wavelengths are

$$\lambda = 1.2, 0.97, 0.84, 0.76 \text{ cm}. \tag{42}$$

Peaks in the spectrum as predicted by this theory have also been encountered during measurements with a wave follower in the ocean during the TOWARD experiment (Shemdin 1986). Only a rough comparison has been made so far, but the locations of the peaks seem to coincide. One possible reason that they were encountered in this experiment but not in others is that spectra are usually measured as a function of frequency. In the ocean short waves ride on long waves. This means that one never measures the intrinsic frequency of the short waves, but always the apparent. Thus all features of the spectrum as a function of wavenumber are smeared out. In the last few years attempts have been made to convert from apparent to intrinsic frequency (Stolte 1984; Ataktürk & Katsaros 1983). However, these were still pretty rough. Shemdin's method based on a matrix conversion seems to be more sophisticated.

From figures 5 and 6 it can be deduced that the viscous decay of the energy level around the main peak of the spectrum is not much faster when nonlinear interactions are taken into account. For $U = 4$ m/s, for instance, about 0.2 times the energy is left at the peak after 3.6 m of fetch in the present model. This is in agreement with the viscous decay factor $\exp(-4\nu k^2 x/c_g)$. This behaviour is in contrast with the prediction of Krasil'nikov & Pavlov (1973); they expect that nonlinear interactions would enhance the decay significantly. The cause of this difference is that they did not anticipate the change in the shape of the spectrum, which greatly reduces the nonlinear interactions for $k < \frac{1}{2}k_0$.

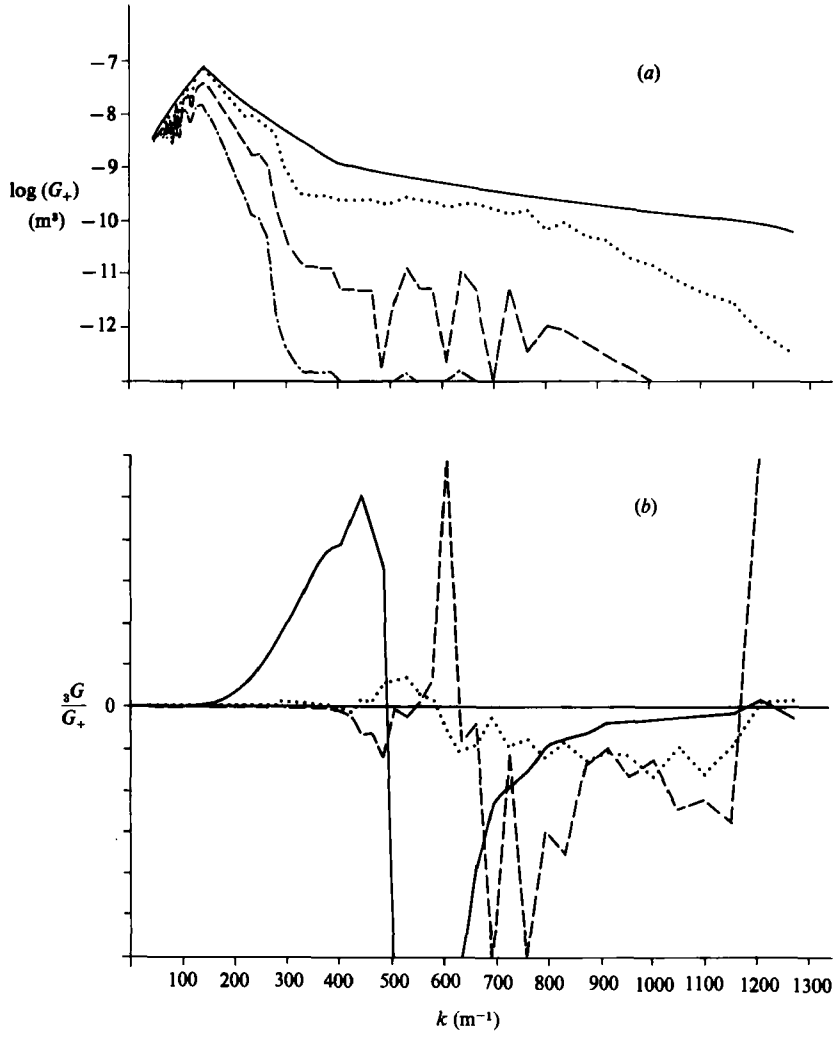

FIGURE 5. The development with fetch of (*a*) the variance spectrum G_+ and (*b*) the third cumulant ${}_3G$ under the influence of nonlinear interactions and viscous damping. The initial state is an approximation of the spectrum measured by Liu & Lin (1982) for a windspeed of 4 m/s. ——, $x = 0$ m; · · · · ·, 0.3 m; – – – –, 1.4 m; –·–·–, 3.6 m.

In figure 7 (*a*) spectra are shown at 0.5 m of fetch, starting with an initial spectrum typical of a wind speed of 4 m/s. The calculations are done on the mixing grid, once with 35 and once with 69 triads. It is seen that the results depend on grid size, both in height of the dips and peaks and in shape of the spectrum around $\frac{1}{2}k_0$. This dependence is found on all mixing grids, because the amount of mixing implicitly present in the model depends on grid size. Thus truly different equations are being solved when the number of bins is changed.

The only grid that does not show this dependence is the one on which no mixing takes place. This grid, constructed in §3, consists of sets $K(k^0)$, $k^0 \in (\frac{1}{2}k_0, k_0]$. Figure 7 (*b*) shows spectra, computed on this non-mixing grid, for the same situation as in figure 7 (*a*). Results for grids consisting of 33 and 66 triads are shown. The results are practically independent of grid size.

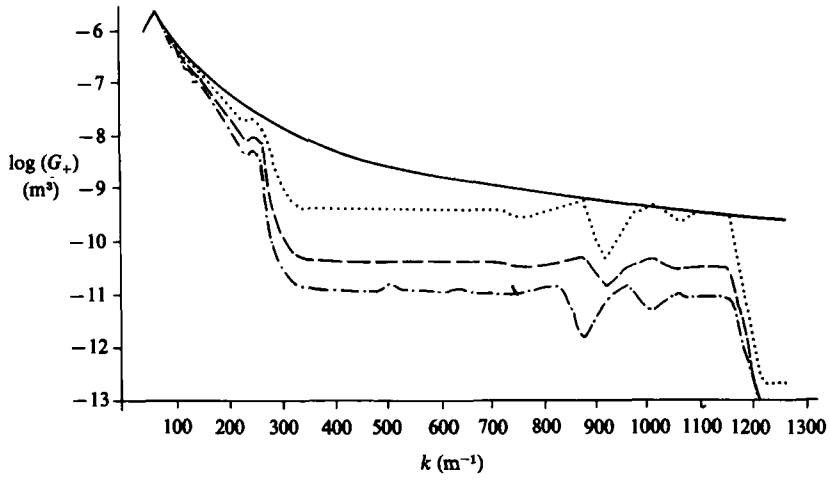

FIGURE 6. As figure 5(*a*), but the initial state measured at $U = 7$ m/s. ——, $x = 0$ m; · · · · ·, 0.4 m; – – – –, 0.9 m; –·–·–, 1.3 m.

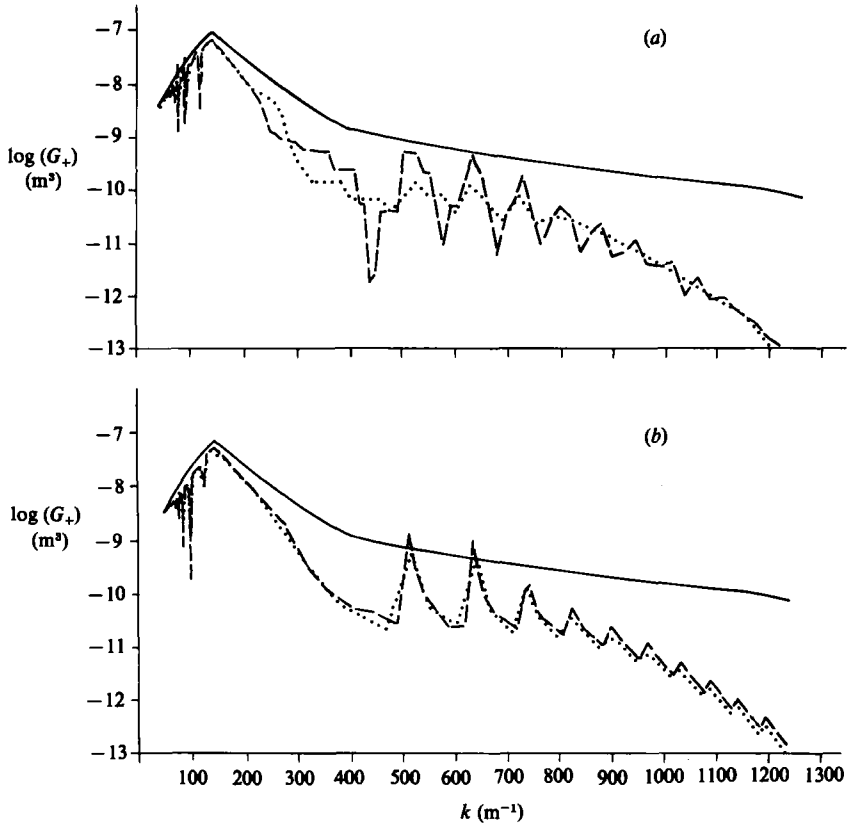

FIGURE 7. Spectra of a fetch of 0.5 m, developed from the initial state as in figure 5 under influence of nonlinear interactions and viscous damping. The calculations are performed: (*a*) on the mixing grid, consisting of · · · · ·, 35 triads; – – – –, 69 triads; (*b*) on the non-mixing grid, consisting of · · · · ·, 33 triads; – – – –, 66 triads. It is only on the non-mixing grid that the results are independent of grid size.

Comparisons of the two types of grids at about 35 triads show that the non-mixing grid has higher peaks and dips, as might be supposed. For about 70 triads this is not yet apparent at a fetch of 0.5 m, but it becomes so at larger fetches. Though mathematically the non-mixing grid is undoubtedly the best to solve (1) these high peaks are disturbing. Further, one may question whether this equation is a good description of nature. In nature diffusive terms, which cause mixing of the sets, are always present, for instance the refraction caused by the orbital motion of gravity waves. Even a very small-amplitude wave causes a lot of mixing: a wave of $\lambda = 1$ m and $ka = \pm 0.003$ gives the same spectra as the mixing grid with 35 triads. For this reason I expect a mixing grid with about 35 triads to give a more realistic description than a non-mixing grid.

In figure 5 not only is the development of the second cumulant, i.e. the spectrum G_+, shown but also of the ratio of third cumulant to second, ${}_3G/G_+$. Only the stationary components of the third cumulant are considered. For $k \geqslant k_0$ there are two; the largest is shown. The magnitudes of these cumulants have to remain of the same order, or decrease, for the weakly nonlinear theory to be valid. These conditions are seen to hold. In §2 it was mentioned that when only nonlinear interactions work the third cumulant goes to a constant. Figure 5 shows that when a linear term is added, in this case viscous damping, a kind of balance sets in where the third cumulant has small, but finite, values. In a follow-up study (van Gastel 1987) it is shown that other linear terms (wind input and linear dissipation) have the same effect.

7. Conclusions

In this paper the integration of a weakly nonlinear energy balance for gravity–capillary waves is made feasible. Results, and an interpretation, are given for the development of a one-dimensional spectrum of gravity–capillary waves under the influence of nonlinear interactions and a linear term, in this case viscous damping.

Concerns about the violation by nonlinear interactions of near Gaussianity appear to be unfounded. Davidson (1972) has shown that for both three- and four-wave interactions the third cumulant goes to a constant. Linear terms do not destroy this process (see also van Gastel 1987). The results presented in this paper clearly show that nonlinear terms are required to give an adequate description of the development of a gravity–capillary wave spectrum. The timescale of the nonlinear interactions is shorter than that of growth by wind. A barrier to including nonlinear interactions in an energy balance used to be the time-consuming algorithms (Valenzuela & Laing 1972). This barrier has been lowered: the present method for calculating nonlinear transfers is estimated to be an order of magnitude quicker than preceding ones. Previous calculations (Valenzuela & Laing 1972) showed a singularity in the nonlinear transfer. Here, however, it is shown that this does not result in a singularity of the energy spectrum. The singular behaviour of the transfer, at one wavenumber, does generate finite peaks and dips at many related wavenumbers. A simple algorithm is given to calculate these wavenumbers. The height of the peaks and especially the dips is very sensitive to the presence of a diffusive term, refraction for instance. Already for the small refraction such as caused by the oribital velocity of an extremely low-amplitude gravity wave ($ka \approx 3\ 10^{-3}$) the dips disappear and the peaks have a relative height of less than four. The calculations presented in this paper show that one needs to be concerned about grid size affecting the results. The nonlinear interactions link together the energy levels of sets of wavenumbers. These sets, of which there are infinitely many, do not interact among each other. There is one type

of grid that maintains this independence. It is only on this grid that the results do not depend on grid size. Any other grid implicitly mixes the sets. As on these grids the amount of mixing depends on grid size the spectral energy depends on grid size. When a diffusive term is present this mixes the sets and hardly any dependence on grid remains.

A new concept that I introduced is multiwave space. This is a concept comparable with phase space. It enables one to take a new viewpoint to look at nonlinear interactions. From this viewpoint a natural way is discovered to go from a continuous to a discrete representation. From this point it is also easy to see how the energy goes through the spectrum and to estimate the size of the transfer.

This work was supported by the Netherlands Organisation for the Advancement of Pure Research (ZWO). I would like to thank Gerbrand Komen and Wim Verkleij for helpful discussions and Henk Tennekes for comments on an early version of this paper. I also thank Frank Henyey for the clue to the argument on near-Gaussianity.

Appendix A

THEOREM. *If*

$$\omega = (gk + Tk^3)^{\frac{1}{2}}, \tag{A 1}$$

$$k_1 + k_2 = k_3, \tag{A 2}$$

$$\omega_1 + \omega_2 = \omega_3, \tag{A 3}$$

$$k_1 > \tfrac{1}{2}k_0, \tag{A 4}$$

then

$$k_2 < \tfrac{1}{2}k_0. \tag{A 5}$$

Proof. I use a dimensionless notation in which $\omega = (k + \alpha k^3)^{\frac{1}{2}}$ and $\frac{1}{2}k_0 = (\frac{1}{2}\alpha)^{\frac{1}{2}}$. I shall prove that if (A 1), (A 2) and (A 4) are fulfilled while (A 5) is not then (A 3) cannot be fulfilled. In this case

$$((\omega_1 + \omega_2)^2 - \omega_3^2)^2 = k_1 k_2 (4(1 + \alpha k_1^2)(1 + \alpha k_2^2) - \alpha^2 9 k_1 k_2 (k_1 + k_2)^2). \tag{A 6}$$

Inserting

$$k_1 = \tfrac{1}{2}\alpha + \Delta_1, \quad k_2 = \tfrac{1}{2}\alpha + \Delta_2, \quad \Delta_1 > 0, \quad \Delta_2 \geqslant 0$$

gives

$$\begin{aligned}((\omega_1 + \omega_2)^2 - \omega_3^2)^2 = k_1 k_2 \{ & -12\sqrt{2\alpha}(\Delta_1 + \Delta_2) - \alpha[\tfrac{33}{2}(\Delta_1 + \Delta_2)^2 + 22\Delta_1 \Delta_2] \\ & - 2a\sqrt{2\alpha}[\tfrac{9}{4}(\Delta_1 + \Delta_2)^3 + 7\Delta_1 \Delta_2 (\Delta_1 + \Delta_2)] \\ & - a^2[14 D_1^2 \Delta_2^2 + 9(\Delta_1^3 \Delta_2 + \Delta_1 \Delta_2^3)]\}. \end{aligned} \tag{A 7}$$

As the right-hand side of (A 7) is always negative (A 3) cannot be fulfilled.

Appendix B

$$K(k^0) = \bigcup_{i=1}^{n} \{k^i(k^0)\}$$

$$A = (\tfrac{1}{2}k_0, k_0]$$

THEOREM 1. *Let* $k_a, k_b \in A$. *Then* $K(k_a) \cap K(k_b) = \varnothing$ *unless* $k_a = k_b$.

THEOREM 2.

$$\bigcup_{k^0 \in A} K(k^0) = [k_{\min}, k_{\max}].$$

For the proofs of both theorems the set $K(k_0)$, drawn for $k \geqslant k_0$ in figure 2, is considered. The first proof also makes use of the following lemma.

LEMMA. *If* $k_a, k_b \in A$ *then* $k_a \in K(k_b) \Leftrightarrow k_a = k_b$.

Proof of lemma. For any $k_a \in A$ $k^1(k_a) \cap A = \varnothing$ (see Appendix A). By construction it can be shown that for

$$i > 1 \qquad \max\{m(k^i(k_a))\} > \max\{m(k^{i-1}(k_a))\}.$$

Thus 'm can only grow' for $k^0 \in A$. Because for $k > \frac{1}{2}k_0$ $\max\{m(k)\}$ is a monotonously increasing function of k this completes the proof.

Proof of theorem 1. Assume $\exists k: k \in K(k_a) \cap K(k_b)$. Then by constructing $K(k)$ one will find both k_a and k_b, thus $k_a \in K(k_b)$. Then $k_a = k_b$ by the lemma.

Proof of theorem 2. Take any $k \in [k_{\min}, k_{\max}]$ for k resp. smaller or larger than $\frac{1}{2}k_0$, find the smallest r for which there exists a $k^r(k_0) \geqslant k$, resp. $k^r(k_0) \leqslant k$ (possible because $K(k_0)$ is discrete). Because the construction of K consists of horizontal and vertical lines and because triads with two members smaller than $\frac{1}{2}k_0$ do not exist (see Appendix A) $\exists k^0 \in A: k \in \{k^r(k^0)\}$.

REFERENCES

ATAKTÜRK, S. S. & KATSAROS, K. B. 1986 Intrinsic frequency spectra of short gravity–capillary waves obtained from temporal measurements of wave height on a lake. *University of Washington.*

BANNER, M. L. & PHILLIPS, O. M. 1974 On the incipient breaking of small scale waves. *J. Fluid Mech.* **65**, 648–656.

BRETHERTON, F. P. 1964 Resonant interactions between waves. The case of discrete oscillations. *J. Fluid Mech.* **20**, 457–479.

DAVIDSON, R. C. 1972 *Methods in Nonlinear Plasma Theory.* Academic.

GASTEL, K. VAN 1987 Imaging by X-band radar of bottom topography and internal waves: a nonlinear phenomenon. *J. Geophys. Res.* (to be published).

GASTEL, K. VAN, JANSSEN, P. A. E. M. & KOMEN, G. J. 1985 On phase velocity and growth rate of wind-induced gravity–capillary waves. *J. Fluid Mech.* **161**, 199–216.

GUCKENHEIMER, J. & HOLMES, P. 1983 *Nonlinear Oscillations, Dynamical Systems, and Bifurcations of Vector Fields.* Springer-Verlag (Appl. math. sciences 42.)

HASSELMANN, K. 1962 On the non-linear energy transfer in a gravity wave spectrum. Part I. *J. Fluid Mech.* **12**, 481–500.

HASSELMANN, K. & HASSELMANN, S. 1981 A symmetrical method of computing the nonlinear transfer in a gravity wave spectrum. *Hamburger Geophysikalische Einzelschriften*, A–52.

HENYEY, F. S. 1983 Hamiltonian description of stratified fluid dynamics. *Phys. Fluids* **26**, 40–47.

HENYEY, F. S. & POMPHREY, N. 1982 Canonical (Feynman diagram) versus non-canonical (Stokes expansion) calculation of resonant interaction between surfaces waves. *Center for Studies of Nonlinear Dynamics, La Jolla.*

HOLLIDAY, D. 1977 On nonlinear interactions in a spectrum of inviscid gravity–capillary surface waves. *J. Fluid Mech.* **83**, 737–749.

KOMEN, G. J., HASSELMANN, S. & HASSELMANN, K. 1984 On the existence of a fully-developed wind–sea spectrum. *J. Phys. Oceanogr.* **14**, 1271–1285.

KRASIL'NIKOV, V. A. & PAVLOV, V. I. 1973 The interaction of random waves on a liquid surface. *Izv. Atm. Ocean. Phys.* **9**, 172–177.

LIU, H. T. & LIN, J. T. 1982 On the spectra of high-frequency wind waves. *J. Fluid Mech.* **123**, 165–185.

LONGUET-HIGGINS, M. S. 1976 On the nonlinear transfer of energy in the peak of a gravity-wave spectrum: a simplified model. *Proc. R. Soc. Lond.* A **347**, 311–328.

LONGUET-HIGGINS, M. S. & SMITH, M. D. 1966 An experiment on third-order resonant wave interactions. *J. Fluid Mech.* **25**, 417–435.

LUKE, J. C. 1967 A variational principle for a fluid with a free surface. *J. Fluid Mech.* **27**, 395–397.

MCGOLDRICK, L. F. 1970 An experiment on second-order capillary gravity resonant wave interactions. *J. Fluid Mech.* **40**, 251–271.

MCGOLDRICK, L. F., PHILLIPS, O. M., HUANG, M. E. & HODGSON, T. H. 1966 Measurements of third-order resonant wave interactions. *J. Fluid Mech.* **25**, 437–456.

MEISS, J. & WATSON, K. 1978 Discussion of some weakly nonlinear systems in continuum mechanics. *AIP Conf. Proc.* vol. 46. American Institute of Physics, NY.

MILES, J. W. 1962 On the generation of surface waves by shear flows. Part 4. *J. Fluid Mech.* **13**, 433–448.

MILES, J. W. & SALMON, R. 1985 Weakly dispersive nonlinear gravity waves. *J. Fluid Mech.* **157**, 519–531.

PHILLIPS, O. M. 1977 *The Dynamics of the Upper Ocean*, 2nd edn. Cambridge University Press, Cambridge.

PHILLIPS, O. M. 1984 On the response of short ocean wave components at a fixed wavenumber to ocean current variations. *J. Phys. Oceanogr.* **14**, 1425–1433.

PLANT, W. J. 1979 The gravity–capillary wave interaction applied to wind-generated, short-gravity waves. *NRL, Washington DC, rep.* 8289.

PLANT, W. J. 1980 On the steady-state energy balance of short gravity wave systems. *J. Phys. Oceanogr.* **10**, 1340–1352.

SHEMDIN, O. H. 1986 'Toward 84/86' field experiment. Investigation of physics and synthetic aperture radar in ocean remote sensing. *Interim Rep. Ocean Sciences Division, Office of the Chief of Naval Research, Arlington, Virginia.*

SIMMONS, W. F. 1969 A variational method for weak resonant wave interactions. *Proc. R. Soc. Lond.* A **309**, 551–575.

STOLTE, S. 1984 Modulation des kurzwelligen Seegangs durch langwelligen Seegang und Wind. *FWG-Bericht* 1984–6.

VALENZUELA, G. R. 1976 The growth of gravity–capillary waves in a coupled shear flow. *J. Fluid Mech.* **76**, 229–250.

VALENZUELA, G. R. & LAING, M. B. 1972 Nonlinear energy transfer in gravity–capillary wave spectra, with applications. *J. Fluid Mech.* **54**, 507–520.

WHITHAM, G. B. 1967 Variational methods and applications to water waves. *Proc. R. Soc. Lond.* A **299**, 6–25.

WILLEBRAND, J. 1975 Energy transport in a nonlinear and inhomogeneous random gravity wave field. *J. Fluid Mech.* **70**, 113–126.

ZAKHAROV, V. E. 1968 Stability of periodic waves of finite amplitude on the surface of a deep fluid. *Zh. Prikl. Mekh. i Tekh. Fiz.* **9**, 68–94.